

Self-Driven Particle Model for Mixed Traffic and Other Disordered Flows

Venkatesan Kanagaraj^a, Martin Treiber^{a,*}

^a*Technical University of Dresden, Germany*

Abstract

Vehicles in developing countries have widely varying dimensions and speeds, and drivers tend to not follow lane discipline. In this flow state called “mixed traffic”, the interactions between drivers and the resulting maneuvers resemble more that of general disordered self-driven particle systems than that of the orderly lane-based traffic flow of industrialized countries. We propose a general multi particle model for such self-driven “high-speed particles” and show that it reproduces the observed characteristics of mixed traffic. The main idea is to generalize a conventional acceleration-based car-following model to a two-dimensional force field. For in-line following, the model reverts to the underlying car-following model, for very slow speeds, it reverts to an anisotropic social-force model for pedestrians. With additional floor fields at the position of lane markings, the model reverts to an integrated car-following and lane-changing model with continuous lateral dynamics including cooperative aspects such as zip merging. With an adaptive cruise control (ACC) system as underlying car-following model, it becomes a controller for the acceleration and steering of autonomous vehicles in mixed or lane-based traffic.

Keywords: Social Forces; Disordered Traffic; Self-Driven Particles; Two-dimensional Traffic Flow; Autonomous Vehicles; Bike Traffic

1. Introduction

Traffic flow in developing countries is growing disproportionately fast now accounting for 80% of the total road accidents and an estimated economic loss of 1-2% of the GNP [1]. As visualized in Fig. 1, vehicles in developing countries have widely varying dimensions and speeds, and drivers tend to not follow lane discipline. In addition to in-line car following (Fig. 1a), a model for mixed traffic should describe staggered following (Fig. 1b), following between two vehicles (Fig. 1c) and passing (Fig. 1d) [18, 10]. Generally, the interactions between drivers and the resulting maneuvers in this flow state, called “mixed traffic”, can only be described fully two-dimensionally. In a wider context, mixed traffic becomes also increasingly relevant in industrialized countries: On the one hand,

*Corresponding author

Email addresses: vkanagaraj.iitm@gmail.com (Venkatesan Kanagaraj), martin@mtreiber.de (Martin Treiber)



Figure 1: The four driving behavioral patterns of mixed traffic. (a) In-line car following, (b) staggered following, (c) following between two vehicles, and (d) passing.

bicycle traffic and its interaction with driving and standing cars and pedestrians has the attributes of mixed traffic, particularly on bike lanes allowing several cyclists to drive in parallel while only single-file bicycle traffic has been modelled [23, 7]. On the other hand, the concept of "shared space" creates mixed traffic (of motorized vehicles, bicycles, and pedestrians) by design [19].

The core behavioral models such as car-following models [2, 13, 1, 21] and lane-changing models [3, 6, 12, 15, 20, 17] are designed for lane-based traffic, only. There exist a few models describing staggered car following [14, 9, 4], or continuous lane changing based on a constant lateral speed [16]. To our knowledge, there are no models describing the full dynamics of non-lane based traffic. Existing self-driven particle models like the social-force model for pedestrians do not apply because, due to the kinematic constraints of high speeds and the negative consequences of crashes, drivers behave qualitatively differently as pedestrians or point-like particles.

In this contribution, we propose a continuous, fully two-dimensional microscopic model for motorized and non-motorized vehicles in unidirectional traffic and show that it reproduces the observed characteristics of mixed traffic on arterials in an Indian city. The main idea is to generalize conventional acceleration-based car-following models to a two-dimensional force field. Depending on the underlying car-following model, its pa-

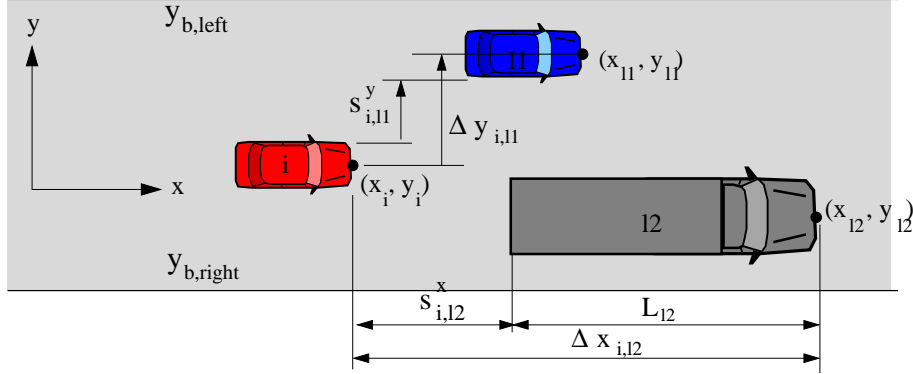


Figure 2: Specification of the geometrical variables of the MTM.

parameterization, and optional floor fields, it can describe manually driven or autonomous motorized vehicles as well as bicycles driving in lane-based and non-lane-based traffic.

Generally, the proposed model describes the directed flow of high-speed self-driven particles where “high-speed” indicates that collisions are undesirable and kinematic aspects such as braking distance play a significant role. This includes all of the above, and the flow of athletes in running and cross-country ski Marathons, city inline-skating events, and others [20, 22].

The paper is organized as follows. In the next two sections, the model is specified and tested for plausibility on some standard situations. In Section 4, the model is calibrated and validated on trajectory data of semi-dense and congested traffic in an Indian city. Section 5 concludes with a discussion.

2. Specification of the Self-Driven-Particle Model

While the Mixed Traffic Flow Model (MTM) proposed in the following is designed to describe general self-driven high-speed particles, we will refer to them as “vehicles”, for notational clarity. Assuming that all considered vehicles drive in the same general direction, we separate the motion into a longitudinal part along the local road axis (coordinate x), and a transversal part perpendicular to it (coordinate y). The transversal dynamics replaces the lane changing component of conventional microscopic traffic flow models. For reasons of simplicity, we consider only rectangular objects (cf. Fig. 2).

We denote the (front-center) position, velocity, and social-force vectors of vehicle i by $\vec{r} = (x, y)$, $\vec{v} = (v, w)$, and $\vec{f} = (f, g)$, respectively. Without loss of generality, we assume all masses $m_i = 1$ such that the force vectors also denote the accelerations. The total acceleration vector $\vec{f} = d\vec{v}_i/dt$ is given by a superposition of several “social forces” according to

$$\frac{d\vec{v}_i}{dt} = \vec{f}_i^{\text{self}}(\vec{v}_i) + \vec{f}_i^{\text{int}}(\vec{r}_i, \vec{v}_i, \{\vec{r}_j, \vec{v}_j\}) + \sum_b \vec{f}_{ib}. \quad (1)$$

This expression formally resembles the acceleration equation of the social-force model for pedestrians [5]. It includes the self-driven acceleration \vec{f}_i^{self} , the interacting force

\vec{f}_i^{int} caused by a set $\{j\}$ of neighboring vehicles, and the external forces \vec{f}_{ib} due to road boundaries, red traffic lights, and other constraints. Notice that, in contrast to [5], we will specify these forces such that they are consistent with the kinematic constraints and driver anticipations that are necessary for a collision-free flow of high-speed particles. Because we consider directed particles, the equations of motion for the longitudinal and transversal dynamics are qualitatively different.

2.1. Longitudinal dynamics

In the longitudinal direction x , we only consider the two-body interaction $f_{il'}$ with the mostly interacting leader or neighbor l' and add up the boundary effects of the left and right boundaries and of red traffic lights,

$$\frac{dv_i}{dt} = f_i^{\text{self}} + f_{il'} + \sum_b f_{ib}, \quad l' = \arg \max_l |f_{il}|. \quad (2)$$

The reason why we only consider a single leader is that, otherwise, multiple leaders may lead to a too defensive behavior. This is particularly relevant if several small vehicles such as motorbikes drive in parallel ahead of a big truck. Then, it is reasonable that only the closest and/or slowest leader should determine the truck driver's acceleration or braking reaction.

We derive the self-driven and interaction accelerations from a conventional acceleration-based single-lane car-following (CF) model where the acceleration $a^{\text{CF}}(\Delta x_{il}, v_i, v_l)$ of the follower i is a function of the longitudinal distance $\Delta x_{il} = x_l - x_i$ to the leader l (including the leader's vehicle length) and the speeds v_i and v_l of the subject vehicle and leader, respectively. This includes the Intelligent-Driver Model (IDM) [21] and variants thereof, the Optimal-Velocity Model (OVM) [1], and the Gipps model [2].

In a first step, we decompose the CF acceleration a^{CF} into a free and an interacting part according to

$$a^{\text{CF}}(\Delta x_{il}, v_i, v_l) = a^{\text{CF,free}}(v_i) + a^{\text{CF,int}}(\Delta x_{il}, v_i, v_l), \quad (3)$$

where

$$a^{\text{CF,free}}(v_i) = a^{\text{CF}}(\infty, v_i, v_i), \quad (4)$$

$$a^{\text{CF,int}}(\Delta x_{il}, v_i, v_l) = a^{\text{CF}}(\Delta x_{il}, v_i, v_l) - a^{\text{CF,free}}(v_i). \quad (5)$$

Notice that, for plausible models, the interaction tends to zero when the distance Δx_{il} tends to infinity (cf. [20] for details), so $a^{\text{CF,free}}$ can be calculated at any value for v_l , including v_i .

In a second step, we identify the free acceleration as the self-driven component of (2) and assume the interaction force f_{il}^{int} from a leader l to be that of the underlying car-following model whenever there is a longitudinal overlap, i.e., an uncontrolled approach to the leader will eventually lead to a rear-end collision. This is the case, if the magnitude of the lateral displacement (cf. Fig. 2) $\Delta y_{il} = y_l - y_i$ is less than the average vehicle width $\overline{W}_{il} = (W_l + W_i)/2$. Otherwise, i.e., if there is a lateral gap $s_{il}^y = |\Delta y_{il}| - \overline{W}_{il} > 0$, the interaction decreases exponentially with this gap. Bringing all this together, the free

and vehicle interaction part of the longitudinal MTM acceleration (2) can be expressed in terms of the CF acceleration by

$$f_i^{\text{self}} = a^{\text{CF,free}}(v_i), \quad (6)$$

and

$$f_{il'} = \alpha(\Delta y_{il'}) a^{\text{CF,int}}(\Delta x_{il'}, v_i, v_{l'}), \quad l' = \arg \max_l |f_{il}|, \quad (7)$$

where the attenuation factor

$$\alpha(\Delta y_{il}) = \min \left\{ \exp \left(-\frac{s_{il}^y}{s_0^y} \right), 1 \right\}, \quad s_{il}^y = |\Delta y_{il}| - \overline{W}_{il} \quad (8)$$

contains the lateral “attenuation scale” s_0^y as a model parameter which can also be interpreted as a “soft” minimum lateral gap (cf. Table 2). Notice that for sufficiently aligned leader-follower pairs with a lateral overlap, $s_{il}^y < 0$, the expressions (6) and (7) reduce to the CF acceleration of the immediate (mostly interacting) leader, i.e., the model reverts to the underlying CF model. To ensure that situations with a longitudinal overlap, i.e., a negative longitudinal gap $s_{il} = x_l - x_i - L_l < 0$ (where L_l is the length of the leader), leads to a consistent behavior, the CF model needs to return its maximum deceleration b_{max} (emergency braking) whenever its distance argument Δx_{il} is less than L_l (i.e., the gap s_{il} is negative).

The external forces f_{ib} can come from road boundaries, red traffic lights and other constraints such as stop signs. A red traffic light or stop sign is modelled as a very short and very wide standing virtual vehicle occupying the complete extension of the stopping line. Notice that these virtual vehicles are considered separately from the real leader, i.e., a follower may brake even if the leader decides to pass the traffic light about to go red. Road boundaries are modelled by decelerating “viscous” shear forces whose influence increases with decreasing lateral gap $s_{ib}^y = \pm(y_b - y_i) - W_i/2$ between vehicle and road boundary (plus/minus for the right/left boundary, respectively) and becomes equal to $-b_b$ if the vehicle touches the road boundary,

$$f_{ib} = -b_b \left(\frac{v_i}{v_0} \right) \exp \left(-\frac{s_{ib}^y}{s_{0b}^y} \right). \quad (9)$$

Notice that (9) is essentially the shear force resulting from (7) with (8) when representing the road boundary by a series of standing virtual vehicles just outside of the road. However, since leaving the designated road surface is typically less harmful than colliding with standing vehicles (at least, if the road has a paved emergency strip), the lateral boundary scale s_{0b}^y should be smaller than s_0^y and the deceleration $-b_b$ when the wheels just touch the boundary is significantly lower than b_{max} . Furthermore, (9) contains another softening factor $\frac{v_i}{v_0}$ allowing to “squeeze” through very narrow bottlenecks at low speeds or partially leave the road when nearly standing. Generally, both road sides exert shear forces according to (9). For very narrow roads, this reduces the speed of the vehicle considerably, even without obstructions from other vehicles.

2.2. Lateral dynamics

According to the general equation (1), the lateral social force or acceleration $g_i = \frac{dw_i}{dt}$ of vehicle i is composed of an external tactical component, road boundary constraints,

and a traffic-dependent component,

$$g_i = g_i^{\text{self}} + g_i^{\text{b}} + g_i^{\text{int}}. \quad (10)$$

The *tactical* component g_i^{self} represents a mandatory or anticipatory lateral displacement (corresponding to lane changes in lane-based traffic) when entering or leaving a road, passing a bottleneck, or simply obeying “drive to the right” or “drive to the left” regulations. Its magnitude (of the order of 1 m/s^2) depends on the urgency of the action. It will not be considered in this paper.

The *road boundary component* has the same functional lateral dependency as the longitudinal component,

$$g_i^{\text{b}} = \pm \tilde{b}_b \left(\frac{v_i}{v_0} \right) \exp \left(-\frac{s_{ib}^y}{\tilde{s}_{0b}^y} \right), \quad (11)$$

where both boundaries are superposed and the “+” sign applies for the left boundary (y is increasing to the right). However, since drivers avoid the road boundary mainly by steering and not by braking, both the magnitude \tilde{b}_b of the lateral acceleration when touching the boundary, and the lateral decay scale \tilde{s}_{0b} are larger than that for the longitudinal force.

The *traffic-dependent interaction component* g_i^{int} is relevant if a driver is obstructed by slower leading vehicles or by vehicles driving closely at the side. Depending on the parameterization, it also reflects to “look back” before initiating right or left movements and perform these maneuvers only if there is no accident risk and no back vehicles are obstructed unreasonably. In our approach, the lateral traffic interaction is mediated by a simple generalized “car-following model” for the lateral coordinates whose “desired lateral speed” reflects the social forces and depends on the surrounding vehicles. However, using a fully fledged CF model for the lateral dynamics (e.g., that used for the longitudinal dynamics) is problematic since CF models only give useful results for forward moving vehicles while lateral motion is symmetric. Particularly, the actual and desired lateral speeds may be negative reflecting a (desire to) move to the left. Moreover, this approach would entail several unnecessary new model parameters.

We therefore consider the simplest model (i) coping with negative speeds and displacements, (ii) taking into account the relevant factors, namely the subject’s lateral speed w_i , the lateral speed w_j of the interacting vehicles j and their lateral displacement $\Delta y = y_j - y_i$, and (iii) fulfilling the plausibility criteria listed in Chapter 11.1 of [20]. Specifically, we consider an OV-like model whose desired lateral speed w_i^0 is mediated by the social forces discussed below,

$$g_i^{\text{int}} = \frac{dw_i^{\text{int}}}{dt} = \frac{w_i^0 - w_i}{\tau}. \quad (12)$$

The model parameter τ denotes the speed adaptation time (cf. Table 2). Furthermore, the heading of the vehicles is restricted to a cone of angle 2θ parallel to the longitudinal direction, i.e., the ratio w/v is restricted by $\pm \tan \theta$. By formulating the lateral acceleration in terms of the OV-like model (12) with the desired lateral speed depending on the interactions rather than formulating the interaction directly, we take into account that the lateral social force does not only depend on the lateral gap to the neighbors but also on the lateral speeds of the considered and interacting vehicles.

Since $w_i^0 = 0$ (corresponding to “drive ahead”) without vehicle-vehicle interaction, we can interpret the contribution $-w_i/\tau$ as the “free” lateral acceleration while the lateral desired speed w_i^0 includes the contributions of all relevant neighbors,

$$w_i^0 = \sum_j w_{ij}^0. \quad (13)$$

Notice that, in contrast to the longitudinal interaction, all neighbors with a relevant interaction are included in order to avoid accidents.

We specify the contribution w_{ij}^0 of an isolated neighboring vehicle j by generalizing the lane-changing model MOBIL [12] to a continuous lateral coordinate. MOBIL states that the *incentive* to change lanes is proportional to the difference between the potential longitudinal acceleration at the new lane and the actual acceleration at the old lane. In the present continuous model, the difference is replaced by the partial derivative of the longitudinal acceleration f_{ij} with respect to y (acceleration shear), so $w_{ij}^0 \propto \partial f_{ij}(x, y)/\partial y$ with $f_{ij}(x, y)$ according to (7). However, for small lateral displacements with an overlap ($|\Delta y| < \overline{W}_{ij}$ or $s_{ij}^y < 0$), this gradient is zero according and a modification is necessary to avoid getting stuck behind a slower vehicle. Assuming that, for this case, the lateral desired speed is proportional to the displacement and that it is a continuous function everywhere, we arrive at following expression for the desired velocity component induced by neighbor j :

$$w_{ij}^0 = \begin{cases} \lambda s_0^y \frac{\partial f_{ij}}{\partial y} & \text{if } |\Delta y_{ij}| \geq \overline{W}_{ij} \\ \lambda f_{ij} \frac{\Delta y_{ij}}{\overline{W}_{ij}} & \text{if } |\Delta y_{ij}| < \overline{W}_{ij} \end{cases}. \quad (14)$$

The new model parameter λ (cf. Table 2) denotes the sensitivity for lateral motion. Specifically, λs_0^y indicates the lateral desired speed induced by a longitudinal acceleration shear of 1 m/s² per meter, and λ itself the maximum ratio between the desired lateral speed and the longitudinal interaction deceleration induced by vehicle j . However, expression (14) still lacks a dependence on the relative lateral speed $w_j - w_i$ which clearly is relevant in order to avoid collisions or prevent unnecessary steering actions. Since such a term cannot be derived from MOBIL, we augment (14) in the simplest possible way that satisfies the plausibility condition “no lateral force if there is no longitudinal force” by adding to (14) a linear relative speed dependence $-\lambda_{\Delta w} \text{sign}(\Delta y_{ij})(w_j - w_i)$ multiplied by (14) itself. The parameter $\lambda_{\Delta w}$ denotes the sensitivity to lateral speed differences (cf. Table 2) and should satisfy $\lambda_{\Delta w} |w_j - w_i| < 1$ for all reasonable relative lateral speeds in order to prevent an implausible driving behavior (lateral “drag-along” effect). Performing the partial derivative on (7) and including the above factor, we obtain following explicit expression for the pair interaction,

$$w_{ij}^0 = \lambda \tilde{\alpha}(\Delta y_{ij}) a_{ij}^{\text{CF}, \text{int}} [1 - \lambda_{\Delta w} (w_j - w_i) \text{sign}(\Delta y_{ij})], \quad (15)$$

where $a_{ij}^{\text{CF}, \text{int}} < 0$ is the interacting part of the (longitudinal) CF acceleration from leader j , and the lateral attenuation factor is given by

$$\tilde{\alpha}(\Delta y_{ij}) = \text{sign}(\Delta y_{ij}) \begin{cases} 1 + s_{ij}^y / \overline{W}_{ij} & s_{ij}^y < 0 \\ \exp(-s_{ij}^y / \tilde{s}_0^y) & s_{ij}^y \geq 0 \end{cases}, \quad s_{il}^y = |\Delta y_{il}| - \overline{W}_{il}. \quad (16)$$

Since drivers prefer steering to braking in order to avoid a collision with another vehicle, we have introduced a different lateral interaction scale \tilde{s}_0^y which is larger than its counterpart s_0^y for the longitudinal accelerations.

The lateral forces are repulsive and increase linearly with the lateral distance in case of a lateral overlap while they decay exponentially, otherwise. Notice that, for the non-overlapping case $s_{ij}^y > 0$ and zero lateral speeds w_i and w_j , the ratio of the longitudinal and lateral repulsive forces (accelerations) from a leading vehicle is given by the dimensionless constant λ/τ .

Expression (15) is only valid for leading neighbors. In order to include followers,

- the role of the leader and follower has to be swapped, i.e., the lateral interaction is calculated for the follower,
- the sign of the contribution has to be swapped, reflecting *actio=reactio*.

In terms of a generalized lane-changing model MOBIL [12], including only the leaders in (13) corresponds to a *politeness factor* $p = 0$ and no active safety criterion, while including all neighbors corresponds to $p = 1$. Obviously, general values of p are realized by weighting the followers with p . For an effective implementation, only leaders and followers are included whose maximum CF interactions exceed a certain threshold, $|a_{ij}^{\text{CF,int}}| > a_{\text{thr}}$ and $|a_{ji}^{\text{CF,int}}| > a_{\text{thr}}$, respectively.

Finally, a safety criterion similar to that of MOBIL is automatically included provided that $p > 0$. This is ensured since we require from the underlying car-following models to return $a^{\text{CF,int}} = -b_{\text{max}}$ whenever the longitudinal gap $s < 0$. This means, the above expressions give a maximum repulsive lateral interaction if neighbors overlap longitudinally with the subject vehicle, i.e. drive nearly in parallel or following very closely or at high speed.

In summary, the complete MTM model is defined by the longitudinal dynamics (2) with (7), (8), (9) and the lateral dynamics (10) with (11), (12), (13), (15), and (16). Typical values of its nine parameters are listed in Table 2. In addition, one needs an underlying CF model whose acceleration output is separable into a free-flow and interacting part.

3. Model Visualization and Plausibility Tests

To visualize the model and test whether it produces plausible driver actions and trajectories, we need to fully specify the model by providing an underlying car-following model. We investigated several well-known models including the Intelligent-Driver Model (IDM) [21], one of its derivatives, the “Adaptive Cruise Control” (ACC) model [11, 20], the optimal-velocity model (OVM) of Bando et al. [1], and the Gipps model [2] in the simplified version presented in [20]. The ACC model can serve as a prototype for the longitudinal control of autonomous vehicles. Unlike the original IDM, it has a triangular fundamental diagram and introduces an additional “coolness factor” preventing the IDM’s unrealistically strong driver response to cut-in maneuvers that regularly happen in mixed traffic, so we will use it as the main underlying model in the calibration and validation in Sec. 4. The remaining dynamical aspects and the parameter set is the same as in the IDM. The OVM is qualitatively different from the ACC and Gipps models since it does not depend on the leader’s speed. Its natural extension, the Full Velocity Difference Model (FVDM) of Jiang et al [8], does not satisfy the basic plausibility conditions of car-following in free and congested traffic (cf. Chapter 11.1 of [20]). This prevents a

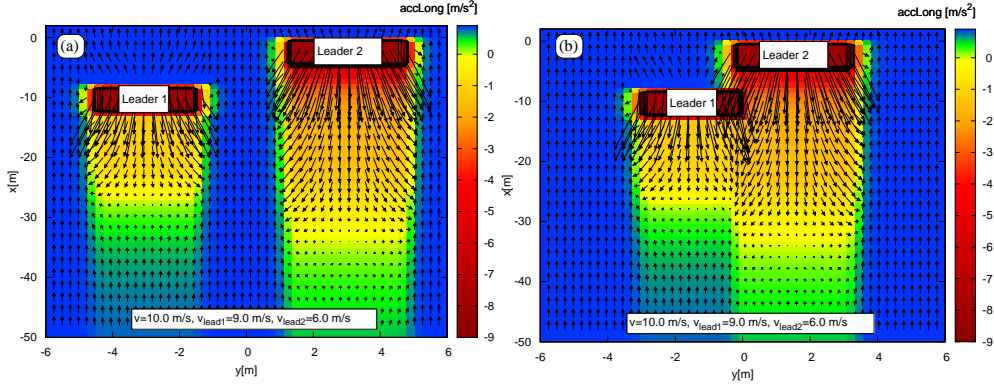


Figure 3: Acceleration vector field of the proposed model for a following vehicle (actual speed $v = 10$ m/s, desired speed $v_0 = 18$ m/s) at arbitrary positions $\vec{r} = (x, y)$ attempting to pass two slower leaders whose outlines are given by the white boxes. Additionally, the longitudinal component is given by the color-coded background. (a) passing between the leaders is possible; (b) the follower needs to circumvent the two leaders. The underlying car-following (CF) model is the ACC model (modified IDM, [11]) with parameters T , s_0 , a and b given in Table 1 for cars. The MTM parameters of the generic MTM particle model are given in Table 2.

decomposition into free and interacting parts according to (4) and (5), so this model is not applicable.

For reference, we use the OVM in the form given in (cf. Chapter 10 of [20])

$$f^{\text{OVM}}(s, v, v_l) = \frac{v_{\text{opt}}(s) - v}{\tau}, \quad v_{\text{opt}}(s) = v_0 \frac{\tanh\left(\frac{s}{\Delta s} - \beta\right) + \tanh \beta}{1 + \tanh \beta}. \quad (17)$$

The Figures 3 and 4 show the acceleration vector field of the MTM as a function of the position (x, y) of the subject vehicle relative to that of two adjacent vehicles. The underlying CF models are the ACC model, the OVM, and the simplified Gipps model in the Figures 3, 4(a)), and 4(b)), respectively. Since the speeds of the other vehicles are significantly below the subject driver's desired speed $v_0 = 20$ m/s, the driver has an incentive to get past them. The MTM acceleration fields reflect following common plausible actions:

- If the other vehicles are leaders and sufficiently far away, or if they are on either side with sufficient lateral space, the acceleration is essentially that on a free road, i.e., positive and in the longitudinal direction.
- in case of a single-lane string of vehicles, the longitudinal part of the MTM reverts to the underlying CF model inheriting all of its properties. particularly, the MTM based on the IDM or the ACC and Gipps models is crash free while that based on the OVM is not.
- If the subject vehicle approaches slower leaders and an action is necessary, the

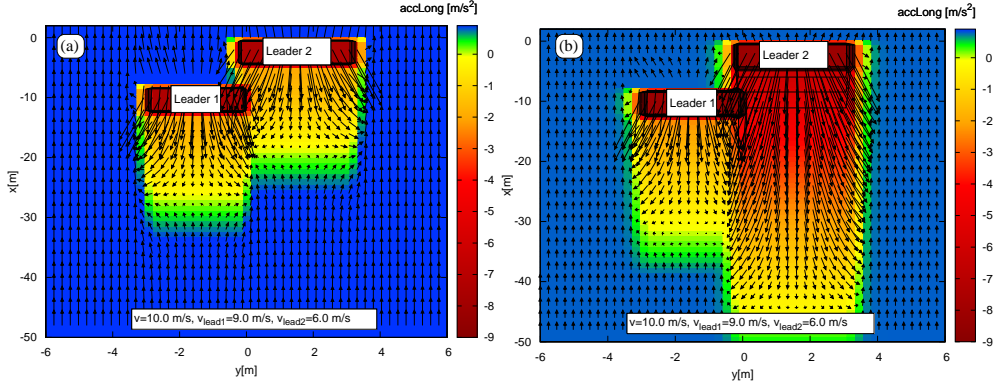


Figure 4: Acceleration vector field as in Fig. 3 (b) for other underlying CF models. (a) OVM [1], Eq. (17); (b) simplified Gipps model as defined in [20]. In both models, the desired speed $v_0 = 18$ m/s. The OVM interaction parameters are $\tau = 5$ s, $\beta = 1$, and $\Delta s = 12$ m. The remaining Gipps model parameters $\Delta t = T$, a , and b are given in Table 1 for cars. The MTM parameters are given in Table 2.

situation is handled by simultaneously decelerating and steering. Depending on the relative position, the acceleration or the steering component prevails.

- If a passage between the leaders is possible, the subject vehicle steers towards the center of the lateral gap and overtakes. Otherwise, the group of the two leaders is circumvented to the right or left. There is also the theoretical possibility that, in a homogeneous stationary situation, a follower gets stuck between leaders driving close together (in Fig. 3(b), it is at $x = -28$ m and $y = -0.7$ m, and in Fig. 4 it is at similar locations). However, the dynamical simulation shows that, in reality, such situations are of a short duration, if they occur at all.

Comparing the underlying models reveals a difference, however: although Leader 2 is further ahead, its braking and steering effect on the follower is stronger compared to that of Leader 1 for the IDM/ACC/Gipps models. The reason is that Leader 2 is slower than Leader 1 and these CF models depend on relative longitudinal speeds. The MTM inherits this property. In contrast, the situation is reversed for the OVM where only gaps matter. Generalizing this, all behavioral aspects (and anticipations) of the underlying CF model carry over to the acceleration, braking and steering strategy of the MTM.

As a further plausibility test, we have simulated, for the IDM/ACC as underlying model, three idealized cases: 1. Passing of an isolated slower vehicle, 2. passing between two slower leaders (Fig. 5(a)), and 3. Circumventing a group of two slower leaders in order to pass (Fig. 5(b)). The simulated drivers display a plausible behavior: first, they move with a lateral component in order to find a suitable gap, then they accelerate to pass the slower vehicles. Notice that the vehicles L1 and L2 hardly react to Vehicle F once it becomes their leader. This plausible behavior is, again, a consequence of the relative speed dependence of the IDM/ACC model producing only little interaction if the leader is faster than the follower. Using the OVM would lead to implausible (too

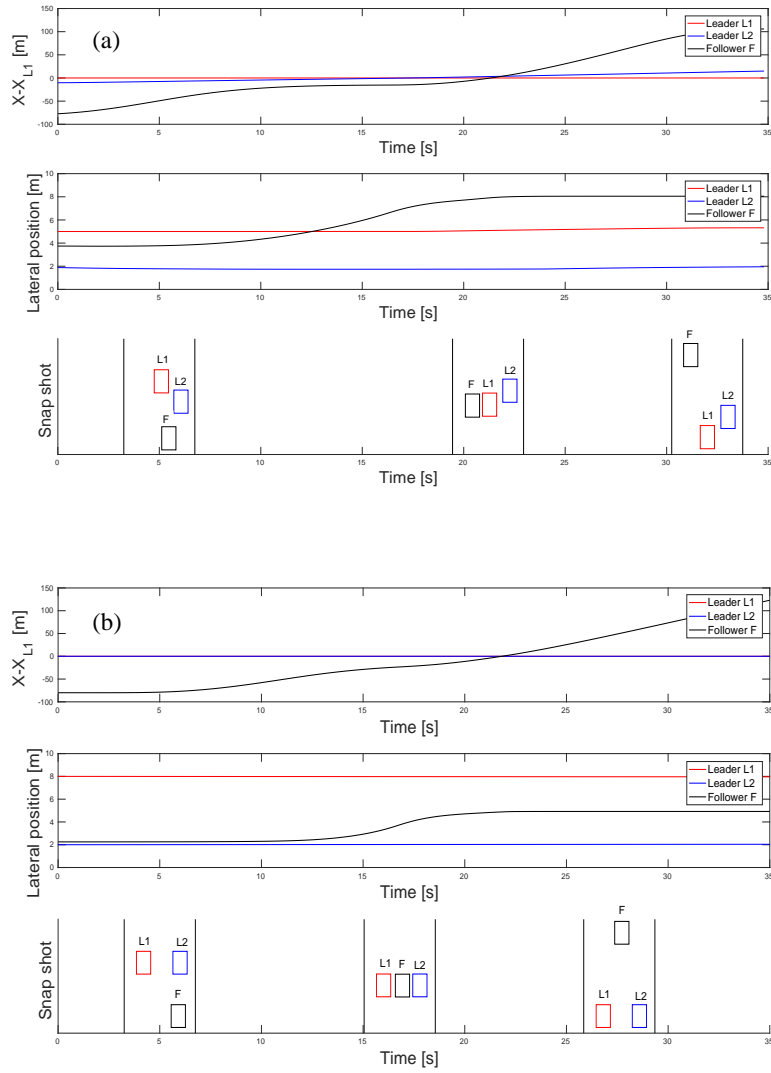


Figure 5: Time series for two passing maneuvers. (a), A follower F passes between two slower leaders L1 and L2. (b), The follower circumvents a group of two slower leaders to the left. Each of the two panels display the longitudinal distance to Leader L1 (top), the lateral position relative to the road axis (middle), and snapshots of the configuration (bottom).

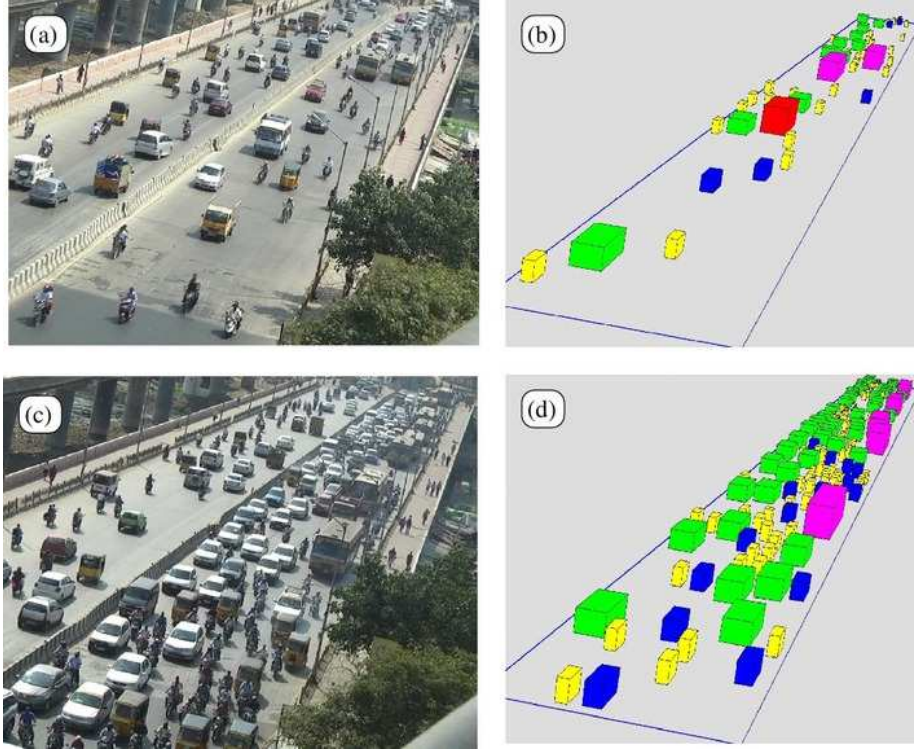


Figure 6: Snapshots and Simulation of mixed traffic. (a), Medium to dense traffic on a 250 m road stretch in Chennai, India. (b), Simulation of this situation with initial conditions taken from the observations. (c)-(d), Observed and simulated congested mixed traffic on the same road. Videos for all four panels are available.

strong) reactions to L1 and L2.

4. Calibration and Validation

In this section, we test the predictive power of the proposed MTM on observed mixed traffic flow in the city Chennai, India. The Panels (a) and (c) of Fig. 6 depict the situation: medium and congested traffic on a 250 m long homogeneous section of a divided urban road with nominal six lanes per roadway. Each roadway has a width of 12 m. See also Supplemental Material Videos 1-4. We only consider the driving direction towards the observer (notice that there is left-hand traffic in India).

In order to calibrate and validate the MTM, we have simulated a 1 500 m long homogeneous section with properties as that of the observation site using the ACC model as underlying car-following model. Initially, the first 250 m (observation section) are populated with the observed vehicle positions and types (motorcycles, cars, busses, and auto-rickshaws) depicted in Fig. 6(a) or Fig. 6(c), respectively, and with initial velocities as derived from the videos. Notice that there were no trucks at the time of recording. From the videos, we have also inferred the typical vehicle dimensions and approximate desired

Table 1: Calibrated ACC model (IDM) parameters for the vehicle mix of the observations shown in Fig. 6. The maximum braking deceleration has always been set to $b_{\max} = 9 \text{ m/s}^2$

Vehicle type	Length [m]	Width [m]	v_0 range [m/s]	T [s]	s_0 [m]	a [m/s^2]	b [m/s^2]
Motorcycle	1.8	0.6	25-18	0.3	0.5	2.0	2.0
Car	4.2	1.7	18-12	0.8	2.0	1.0	1.0
Bus	10.3	2.1	14-10	1.0	2.0	1.0	1.0
Auto-Rickshaw	2.6	0.9	5-6	1.0	2.0	1.0	1.0

Table 2: Calibrated Parameters of the mixed traffic flow model

Parameter	value
maximum angle to road axis θ	0.2 rad
lateral interaction scale for braking s_0^y	0.15 m
lateral interaction scale for steering \tilde{s}_0^y	0.30 m
boundary interaction scale for braking s_{0b}^y	0.15 m
boundary interaction scale for steering \tilde{s}_{0b}^y	0.25 m
lateral sensitivity λ	0.4 s
lateral time constant τ	1 s
sensitivity to lateral relative speeds $\lambda_{\Delta w}$	0.7 s/m
politeness factor p	0.2

Table 3: Observed and simulated characteristics of the mixed traffic flow at the test site in Chennai, India (Fig. 6)

Variables	Observed	Simulated
Calibration-Medium		
Average travel time [s]	7.24	6.16
Travel time standard deviation [s]	3.02	3.90
Entry flow[veh/s]	2.79	2.42
Exit flow[veh/s]	1.96	2.21
Number of lateral shifts	11.00	14.00
Validation-Congested		
Average travel time [s]	12.82	13.41
Travel time standard deviation [s]	7.28	5.95
Entry flow[veh/s]	1.87	1.79
Exit flow[veh/s]	2.31	2.68
Number of lateral shifts	14.00	9.00

speed distributions (Columns 2-4 of Table 1). For illustrative purposes, the 1d partial densities obtained from the video were 170 motorcycles/km, 55 cars/km, 10 buses/km, 15 auto-rickshaws/km for medium traffic, and 450 motorcycles/km, 225 cars/km, 35 buses/km, and 80 auto-rickshaws/km for congested traffic. The rest of the simulated road section is initialized by repeating this configuration until the end of the road is reached.

During the simulation (simulation time 20 s), no additional vehicles were introduced at the upstream boundary while the downstream boundary is free, i.e., vehicles are removed once they cross the downstream boundary resulting in free traffic for the immediate followers. The test section for calibration and validation is in the range $x \in [180 \text{ m}, 227 \text{ m}]$. The road section was long enough such that, during the simulation time, only vehicles defined by the initial conditions could enter the test region, and also traffic waves near the downstream boundary cannot reach the test region, i.e., the boundary conditions do not play a role.

We have calibrated the model on medium traffic (Fig. 6 (a)) by minimizing a mixed objective function consisting of the observed macroscopic characteristics of traffic flow listed in Table 3,

$$S(\vec{\beta}) = \sqrt{\sum_{i=1}^5 \left(\frac{X_i^{\text{sim}}(\vec{\beta}) - X_i^{\text{obs}}}{X_i^{\text{obs}}} \right)^2}, \quad (18)$$

where X_i denotes average travel time through the test section, its standard deviation, the average entry and exit flows into and from the test section, and the total number of “lateral shifts” in this region. A lateral shift event happens if (i) the vehicle moves laterally by more than 1 m in the same direction, and (ii) its leader as defined by (7) changes. The optimization is performed by MATLAB’s standard genetic algorithm. Figure 6 (b) shows a snapshot of the simulation for medium traffic after the calibration. The estimated model parameters are given in the Tables 1 and 2. We observed that all simulated flow characteristics of the calibrated model agree with that of the data to within 20 %

In order to validate the model, we have applied the calibrated model to the congested situation (Figs 6 (c) and (d)). With respect to the calibration, we have only changed the initial vehicle configuration to the observed one keeping all parameters to their calibrated values. Apart from the number of lateral shifts, the other simulated criteria differ less than 20 % from the observations (Table 3). In view of the fact that the validation scenario is qualitatively different (congested rather than medium traffic), this indicates a good predictive power. The difference in the number of lateral shifts is possibly explained by a more aggressive driving behavior in congested traffic, or by additional cooperation, which is not reflected by the model.

5. Concluding Remarks

We have proposed a two-dimensional time-continuous model for mixed traffic flow of motorized and non-motorized vehicles, the mixed traffic flow model (MTM), and tested it on real observations. The MTM generalizes a conventional acceleration-based single-lane car-following (CF) model to two continuous dimensions. Because it is based on a CF model, the MTM can be considered as a framework rather than a specific model. This

means that all behavioral aspects of the underlying CF model carry over to the two-dimensional model: acceleration and steering are intrinsically connected. Methodically, the proposed approach is similar to that leading to the discrete lane-changing model MOBIL [12]. In fact, when introducing additional thresholds or “floor fields” representing lane markers, the model reverts to an integrated car-following and lane-changing model which, unlike MOBIL, models explicit steering maneuvers and also contains, for a politeness factor $p > 0$, cooperative elements such as zipper merging. This will be an interesting research topic for the future. While the MTM is formally similar to the social-force model for pedestrians [5], its basic assumptions (explicit consideration of vehicle kinematics, unidirectional flow, no collisions if the CF model is collision free) are markedly different. We expect that the MTM can serve as a general model platform for “high-speed” self-driven particles and can be parameterized or extended to describe bicycle traffic, acceleration and steering of autonomous vehicles (Markoff, 2010), and crowd flow in mass-sports events (Treiber et al., 2015).

Acknowledgements

The first author is supported by a fellowship of the Alexander von Humboldt Research Foundation, Germany at the Technical University of Dresden, Germany.

References

- [1] M. Bando, K. Hasebe, K. Nakanishi, A. Nakayama, A. Shibata, and Y. Sugiyama. Phenomenological study of dynamical model of traffic flow. *Journal de Physique I France*, 5:1389–1399, 1995.
- [2] P. G. Gipps. A behavioural car-following model for computer simulation. *Transportation Research Part B: Methodological*, 15:105–111, 1981. doi: 10.1016/0191-2615(81)90037-0.
- [3] P. G. Gipps. A model for the structure of lane-changing decisions. *Transportation Research Part B: Methodological*, 20:403–414, 1986. doi: 10.1016/0191-2615(86)90012-3.
- [4] Banihan Gunay. Car following theory with lateral discomfort. *Transportation Research Part B: Methodological*, 41(7):722 – 735, 2007. ISSN 0191-2615. doi: <http://dx.doi.org/10.1016/j.trb.2007.02.002>. URL <http://www.sciencedirect.com/science/article/pii/S0191261507000161>.
- [5] Dirk Helbing and Péter Molnár. Social force model for pedestrian dynamics. *Physical Review E*, 51:4282–4286, 1995.
- [6] Peter Hidas. Modelling lane changing and merging in microscopic traffic simulation. *Transportation Research Part C: Emerging Technologies*, 10:351–371, 2002.
- [7] Serge Hoogendoorn and Winnie Daamen. Bicycle headway modeling and its applications. *Transportation Research Record: Journal of the Transportation Research Board*, 1(2587):34–40, 2016.
- [8] Rui Jiang, Qingsong Wu, and Zuojin Zhu. Full velocity difference model for a car-following theory. *Physical Review E*, 64:017101, 2001.
- [9] Sheng Jin, Dian-Hai Wang, Cheng Xu, and Zhi-Yi Huang. Staggered car-following induced by lateral separation effects in traffic flow. *Physics Letters A*, 376(3):153 – 157, 2012. ISSN 0375-9601. doi: 10.1016/j.physleta.2011.11.005.
- [10] Venkatesan Kanagaraj, Gowri Asaithambi, Tomer Toledo, and Tzu-Chang Lee. Trajectory data and flow characteristics of mixed traffic. *Transportation Research Record: Journal of the Transportation Research Board*, 2491:1–11, 2015. doi: 10.3141/2491-01.
- [11] A. Kesting, M. Treiber, and D. Helbing. Enhanced intelligent driver model to access the impact of driving strategies on traffic capacity. *Philosophical Transactions of the Royal Society A*, 368: 4585–4605, 2010.
- [12] Arne Kesting, Martin Treiber, and Dirk Helbing. General lane-changing model MOBIL for car-following models. *Transportation Research Record*, 1999:86–94, 2007.
- [13] S. Krauß. Microscopic traffic simulation: Robustness of a simple approach. In A. Bachem D.E. Wolf, M. Schreckenberg, editor, *Traffic and Granular Flow '97*, page 269. Springer, Singapore, 1998.

- [14] Tzu-Chang Lee, John Polak, and Michael Bell. New approach to modeling mixed traffic containing motorcycles in urban areas. *Transportation Research Record: Journal of the Transportation Research Board*, 2140:195–205, 2009. doi: 10.3141/2140-22.
- [15] Sara Moridpour, Majid Sarvi, and Geoff Rose. Lane changing models: a critical review. *Transportation Letters*, 2(3):157–173, 2010. doi: 10.3328/TL.2010.02.03.157-173.
- [16] Timothy Oketch. New modeling approach for mixed-traffic streams with nonmotorized vehicles. *Transportation Research Record: Journal of the Transportation Research Board*, 1705:61–69, 2000. doi: 10.3141/1705-10.
- [17] M. Rahman, M. Chowdhury, Y. Xie, and Y. He. Review of microscopic lane-changing models and future research opportunities. *IEEE Transactions on Intelligent Transportation Systems*, 14(4): 1942–1956, 2013. ISSN 1524-9050. doi: 10.1109/TITS.2013.2272074.
- [18] Sandy Robertson. Motorcycling and congestion: Definition of behaviours. *Contemporary Ergonomics*, pages 273–277, 2002.
- [19] Robert Schnauer, Martin Stubenschrott, Weinan Huang, Christian Rudloff, and Martin Fellendorf. Modeling concepts for mixed traffic. *Transportation Research Record: Journal of the Transportation Research Board*, 2316:114–121, 2012. doi: 10.3141/2316-13.
- [20] M. Treiber and A. Kesting. *Traffic Flow Dynamics: Data, Models and Simulation*. Springer, Berlin, 2013. URL <http://www.traffic-flow-dynamics.org>.
- [21] M. Treiber, Ansgar Hennecke, and D. Helbing. Congested traffic states in empirical observations and microscopic simulations. *Physical Review E*, 62:1805–1824, 2000. doi: 10.1103/PhysRevE.62.1805.
- [22] M. Treiber, R. Germ, and A. Kesting. From drivers to athletes – modeling and simulating cross-country skiing marathons. In *Traffic and Granular Flow '13*, pages 243–249, Berlin, 2015. Springer. doi: DOI:10.1007/978-3-319-10629-8_29.
- [23] Jun Zhang, Wolfgang Mehner, Stefan Holl, Maik Boltes, Erik Andresen, Andreas Schadschneider, and Armin Seyfried. Universal flow-density relation of single-file bicycle, pedestrian and car motion. *Physics Letters A*, 378(44):3274–3277, 2014.